

Supporting Information for “Enhanced electrocatalytic activities of pulse-mode potentiostatic electrodeposited single-crystal, fern-like Pt nanorods”

Huei-Yu Chou,^a Ming-Chi Tsai,^a Sung-Yen Wei,^b Yu-Hsuan Wei,^{ad} Tsung-Kuang Yeh,^a
Fu-Rong Chen,^a Chen-Chi M. Ma,^c Chuen-Horng Tsai,^{*a} and Chien-Kuo Hsieh,^{*d}

^a Department of Engineering and System Science, National Tsing Hua University, Hsingchu 30013, Taiwan, ROC.

^b Department of Advanced Optoelectronic Materials and Devices, Industrial Technology Research Institute, Chung 31040, Taiwan, ROC.

^c Department of Chemical Engineering, National Tsing Hua University, Hsingchu 30013, Taiwan, ROC.

^d Department of Materials Engineering, Ming Chi University of Technology, New Taipei City 24301, Taiwan, ROC.; E-mail: jack_hsieh@mail.mcut.edu.tw; d947121@oz.nthu.edu.tw (C. K. Hsieh)

1. Experimental

a. Electrodeposition of Pt nanorods on carbon paper

Electrochemical processes were conducted on untreated carbon papers (CP; size 1 cm², ElectroChem, Inc.). With a three-electrode electrochemical cell, Pt-NR was electrodeposited onto a CP specimen via a pulse-mode potentiostatic electrodeposition (PPE) technique, with a high potential of 1.2 V_{SCE} and low potential of -0.24 V_{SCE}. The frequency between high and low potentials was 1.67 Hz for 480 cycles. A Pt mesh served as the counter electrode and a saturated calomel electrode (SCE) was used as the reference electrode. The electrodeposition electrolyte was 0.2 mM H₂PtCl₆·6H₂O (Alfa Aesar®) + 0.1 M H₂SO₄ (95-97%, J. T. Baker). The deposition electrolytes were saturated with Ar during the deposition processes conducted under ambient pressure and a controlled temperature of 30 °C. After the electrodeposition procedures, the prepared specimens were thoroughly rinsed and reserved in 0.5 M H₂SO₄ aqueous solution. Fig. 1 shows a wide view SEM image of Pt-NR on CP.

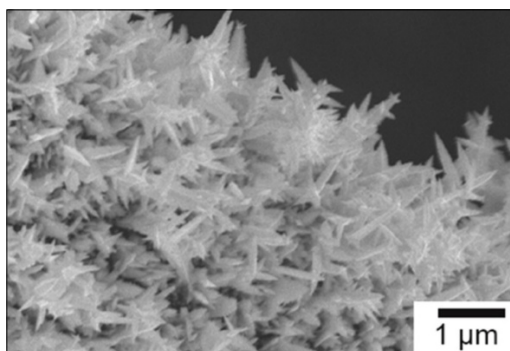


Fig. 1 A wide view SEM image of our directly synthesized Pt-NR on carbon paper.

For comparison, a commercial Pt-black catalyst (E-Tek, XC-72, Alfa Aesar®) was also deposited onto a CP specimen. The catalysts were first mixed with Nafion solution. The resulting slurry ink was then sprayed onto the CP. Fig. 2 shows the TEM of Pt black.

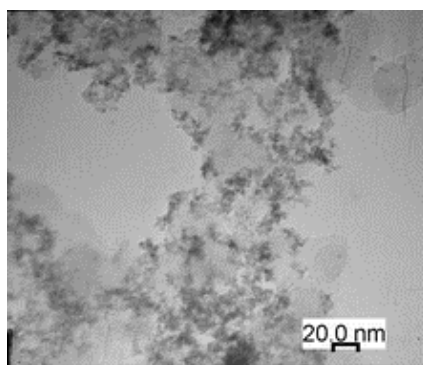


Fig. 2 TEM image of the Pt black.

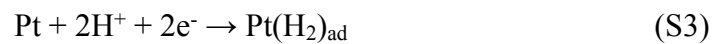
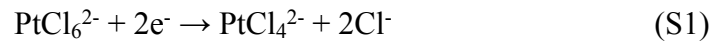
b. Electrochemical and structural analyses of Pt nanorods

Before the catalytic efficiencies test, each specimen was analyzed by CV at a scan rate of 20 mV s⁻¹ with potentials ranging from -0.2 to 0.35 V_{SCE} for five cycles in an Ar saturated 0.5 M H₂SO₄ aqueous solution. The CV analyses for evaluating the catalytic efficiencies of prepared specimens were conducted at a scan rate of 20 mV s⁻¹ with potentials ranging from -0.2 to 0.9 V_{SCE} for five cycles. The test solutions were Ar saturated 0.5 M H₂SO₄ with 1 M CH₃OH (99%, Union Chemical Works LTD., Hsinchu), 0.1 M HCHO (24%, First Chemical Works, Taipei), and 0.1 M CH₂O₂ (≥98%, Sigma-Aldrich), respectively.

All electrochemical operations were performed on an Autolab PGSTAT 302N potentiostat. The morphologies and structures of the electrodes were analyzed with a JEOL JSM-6330F SEM, a JEM-2100F TEM, a JEM-2100 TEM. Pt loadings were measured by an inductively coupled plasma-mass spectrometer, ICP-MS (SCIEX ELAN 5000, Perkin Elmer).

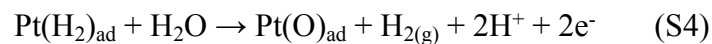
The surface structure of Pt metals can be modified by adsorbed oxygen-like species at high positive potentials.¹ In our study, we propose the mechanism of a continuously sequence of reactions involving nucleation/growth and the structural modification of Pt.

The following possible reactions might occur during PPE at negative potentials.²

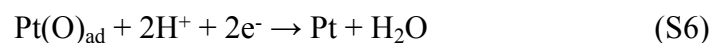


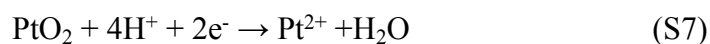
In addition to reactions (S1) and (S2), the adsorption of hydrogen bubbles might also occur at standard hydrogen reduction reaction (SHRR, -0.241 V_{SCE}, eqn (S3)) potential, there were considerable hydrogen bubbles accumulated on Pt surfaces at applied potential below -0.241 V_{SCE}.

At the higher positive potential (1.2 V_{SCE}), following reaction might occur:²⁻⁵



Reaction (S4) suggests that the desorption of hydrogen bubbles may occur by the reaction with H₂O. However, reaction (S5) would occur without hydrogen adsorption on Pt surfaces. And then, eqn S5 and S6 might also occur. After that, at a low negative potentials, reactions (S6) - (S8) have been suggested, resulting in the formation of pure Pt metal.²





2. Electrochemical Analysis

a. Electrochemical Surface Activity (ECSA, or ESA), and Specific Activity (SA)

Figure 3 shows a typical ECSA (or ESA) measurement. The ECSA calculation is based on several assumptions, particularly that the H adsorption/desorption charge density on polycrystalline Pt is $210 \mu\text{C cm}^{-2} \text{Pt}$, derived from equal distribution of the three low index planes (111), (110) and (100) of Pt. Commonly, it is used for catalyst evaluation in fuel cell. The equation used to calculate ECSA shows as Eq. R1.^{6,7} The specific activity (SA) is the current divided by real surface area.

$$\text{ECSA} = \frac{Q_{\text{H}}}{[\text{Pt}] \times 0.21} \quad (\text{Eq. R1})$$

Where the [Pt] is the Pt loading (mg cm^{-2}), Q_{H} is the charge for hydrogen desorption (mC cm^{-2}), 0.21 is the charge required to oxidize a monolayer of hydrogen on bright Pt.

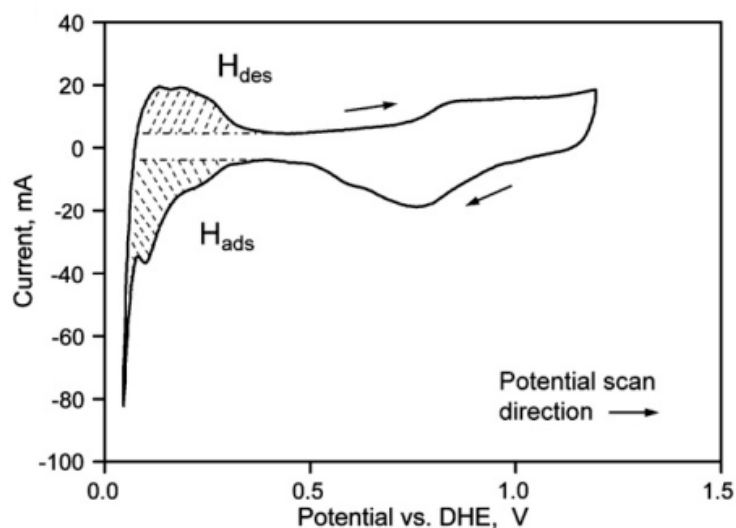


Fig. 3 A typical I-V curve of ECSA analysis.⁷

b. Voltammograms corresponding to (110), (100), and (111) of Pt

Fig. 4 shows the voltammograms of electrode surfaces having low-Miller-indices of Pt. Each of

these surfaces gives it proper voltammogram characteristic for the Pt atomic arrangement in it.

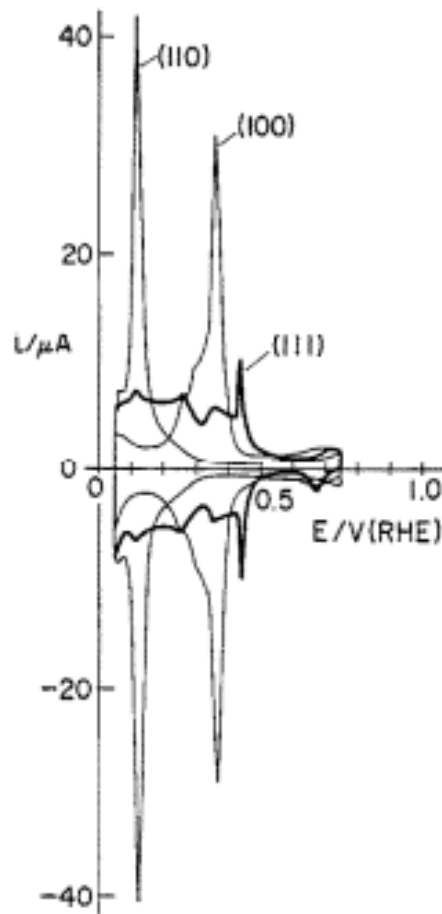


Fig. 4 Voltammograms for the (110), (100), and (111) of Pt.⁸

c. Electrochemical characteristics of our prepared Pt-NR and Pt black.

Table 1 shows the electrochemical characteristic, the calculation methods shown as below equations:

$$MA = \frac{i_f}{\text{loading}}$$

$$SA = \frac{i_f}{ECSA}$$

$$SVR = \frac{MA}{SA}$$

In general, the surface-to-volume ratio (SVR) is related to the size of Pt nanoparticle. The higher the Pt loading on electrode, the bigger the size of Pt particle. It can be realized simply that too many

ineffective Pt atoms inside particle which are unexposed to methanol to occur catalytic effect. As particle size shrink to nano-scale, the effective catalytic Pt atoms will be increased sharply. From Table 1, our SVR of Pt-NR is smaller of those of Pt-black. However, the SA of Pt-NR is more 10.54 times than Pt black. We suggest that Pt-NR is Pt(110) rich in ECSA plot which can boost the catalytic efficiencies.

Table 1 Electrochemical characteristics of our prepared Pt-NR and Pt black.

Sample	Loading (mg/cm ²)	i_f (mA/cm ²)	ECSA (cm ²)	MA (mA/mg _{Pt})	SA (mA/cm ² _{Pt})	SVR (cm ² /cm ³) X 10E6
Pt-NR	0.55	195	21.58	354.55	9.036	0.84
Pt black	0.65	54	63.00	83.08	0.857	2.08

MA: mass activity, SA: Surface activity, SVR: Surface to volume ratio.

3. Pt atoms and their configuration

Fig.5 shows the Pt atomic distance at various planes and directions. Fig.6 shows the distance between neighboring hydrogen of various fuels. As we can see in the Fig.5, the Pt atomic gap of [110] at (100), (110) and (111) are all 0 Å, which means that the neighbouring hydrogen of the fuel (as shown in Fig.6) may be decomposed the hydrogen on the atoms of Pt[110]. The capability of hydrogen decomposing will decrease following the increasing gap of Pt atoms. For example, the H₁H₂ of CH₃OH may not be decomposed on the atoms of Pt[100], because the distance of neighbouring hydrogen (H₁H₂ of CH₃OH is 0.7277 Å, Fig 6(a)) is smaller than the gap distance of Pt[100] (1.149 Å). A higher poisoning effect may occur on Pt(111) due to its zero gap, by another word, a lower poisoning effect may occur on the Pt(110) due to its larger atomic gap of [100] and [211].

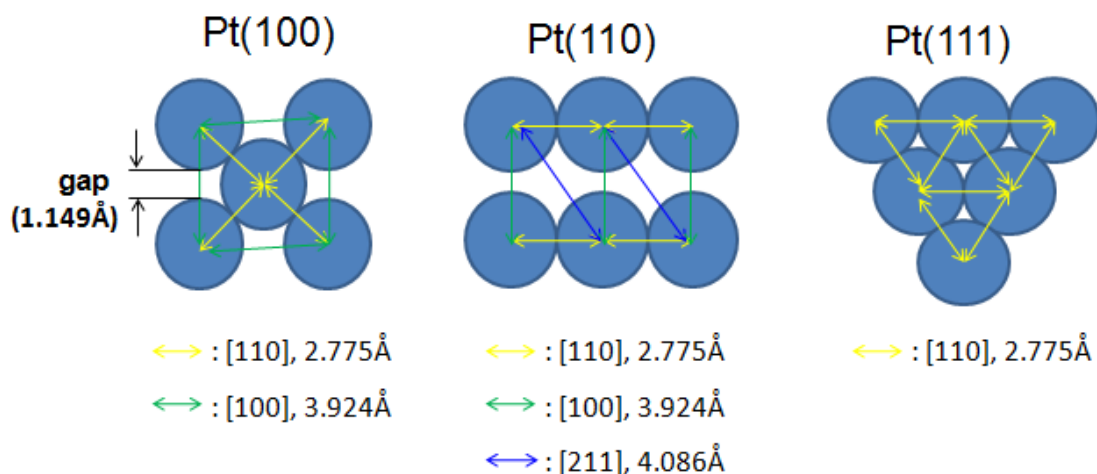


Fig. 5 The atomic distance between Pt atoms at various planes and directions.

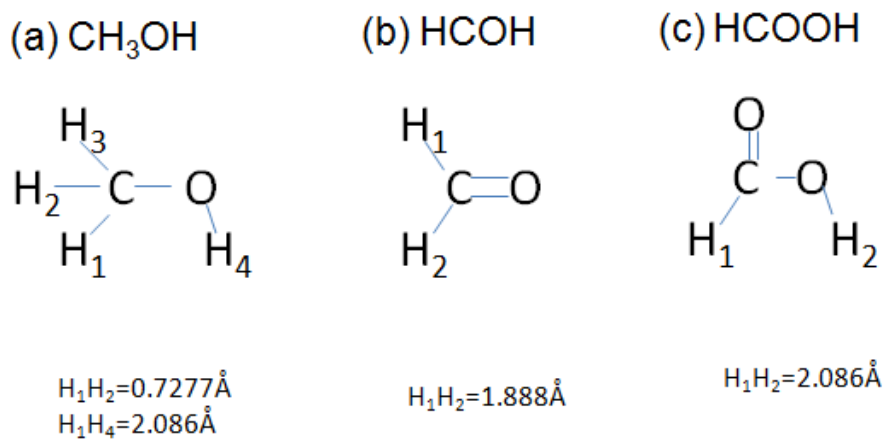


Fig. 6 The distance between neighbouring hydrogen of (a) methanol, (b) formaldehyde, and (c) formic acid.

References

1. B. E. Conway, *Prog Surf Sci*, 1995, **49**, 331-452.
2. D. R. Lide, *CRC handbook of Chemistry and Physics*, CRC Press, Cleveland, 2002.
3. B. E. Conway, *Journal of Electroanalytical Chemistry*, 2002, **524**, 4-19.
4. V. I. Birss, M. Chang and J. Segal, *Journal of Electroanalytical Chemistry*, 1993, **355**, 181-191.
5. G. Jerkiewicz, G. Vatankhah, J. Lessard, M. P. Soriaga and Y. S. Park, *Electrochimica Acta*, 2004, **49**, 1451-1459.

- 6.A. Pozio, M. De Francesco, A. Cemmi, F. Cardellini and L. Giorgi, *Journal of Power Sources*, 2002, **105**, 13-19.
- 7.W. Li and A. M. Lane, *Electrochemistry Communications*, 2011, **13**, 913-916.
- 8.N. Furuya and S. Koide, *Surf Sci*, 1989, **220**, 18-28.